Anal. Chem. **1999,** *71,* 3206−3218

Fragmentation Reactions in the Mass Spectrometry Analysis of Neutral Oligosaccharides

Mark T. Cancilla, Anissa W. Wong, Lisa R. Voss, and Carlito B. Lebrilla*

Department of Chemistry, University of California, Davis, California 95616

A method is described to obtain multicollision dissociation threshold (MCDT) values. These values provide relative reaction thresholds for dissociation in the three major gas-phase fragmentation reactions of oligosaccharides complexed to alkali metal ions. The quasimolecular ions are produced using matrix-assisted laser desorption/ionization Fourier transform mass spectrometry. The MCDTs for alkali metal ion dissociation and glycosidic bond and cross-ring cleavages were resolved from the kinetic energy dependence of collision-induced dissociation (CID) products. The relative strengths of alkali metal ion binding to *N*,*N*′-diacetylchitobiose (chitobiose) and *N*,*N*′,*N*″-triacetylchitotriose (chitotriose) were probed using sustained off-resonance irradiation (SORI) CID. Experiments to evaluate MCDT values and the method for obtaining them were performed by studying alkali metal ion coordinated crown ethers. Molecular dynamic simulations were also performed to provide insight into the alkali metal ion binding of chitin-based oligosaccharides. The relative dissociation thresholds of glycosidic bond cleavages and cross-ring cleavages were determined for various alkali metal ion coordinated oligosaccharides. The activation barriers of glycosidic bond cleavages were found to depend on the size of the alkali metal ion. Cross-ring cleavages were found to be independent of the alkali metal ion but dependent on linkage type. The results suggest that glycosidic bond cleavages are charge-induced while cross-ring cleavages are charge-remote processes.

The development of matrix-assisted laser desorption/ionization (MALDI)[1,2] has produced one of the most sensitive and rapid analytical methods for studying oligosaccharides.[3−10] The ionization method provides high sensitivity, allowing mass spectrometry to play a greater role in oligosaccharide analysis. Oligosaccharide "quasimolecular" ions produced by MALDI are often alkali metal ion coordinated species.[3,6−8,10−14] Oligosaccharides appear to be strong ligands for alkali metal ions. With few exceptions, the quasimolecular ion is a complex of the oligosaccharide and Na^+. The comparison of fragment ions produced by collision-induced dissociation shows a marked difference between protonated and sodiated oligosaccharides.[15,16] Protonated oligosaccharides fragment to produce mainly glycosidic bond cleavages. Alkali metal ion coordinated oligosaccharides provide a richer variety of fragments, including cross-ring cleavages that are indicative of linkages. The strength of the interactions between cations and oligosaccharides can play an important role in the intensity of the quasimolecular ions. A strongly bound cation will increase the sensitivity but apparently at the expense of the intensity of the quasimolecular ions. For example, a strongly bound cation such as Li^+ produces a greater degree of fragmentation than Cs^+, which is not as strongly bound, under identical ionization conditions.[6] The yield of structurally informative fragment ions during MALDI and collision-induced dissociation (CID) appears to depend on the strength of the metal−oligosaccharide interactions.[6,17] For analysis, it is important to know, a priori, which alkali metal ions produce the most structurally informative fragments and which will produce primarily molecular ions.

The three dominant processes in the fragmentation of an alkali metal ion (e.g., Na^+) coordinated oligosaccharide are the loss of the metal ion (pathway A, Scheme 1), glycosidic bond cleavage (pathway B), and cross-ring cleavage (pathway C; fragmentation of $C_2H_4O_2$ is represented).[18−27] The roles of the alkali metal ions

(1) Karas, M.; Hillenkamp, F. *Anal. Chem.* **1988**, *60*, 2299−301.
(2) Karas, M.; Ehring, H.; Nordhoff, E.; Stahl, B.; Strupat, K.; Hillenkamp, F.; Grehl, M.; Krebs, B. *Org. Mass Spectrom.* **1993**, *28*, 1476−81.
(3) Harvey, D. J.; Rudd, P. M.; Bateman, R. H.; Bordoli, R. S.; Howes, K.; Hoyes, J. B.; Vickers, R. G. *Org. Mass Spectrom.* **1994**, *29*, 753−66.
(4) Harvey, D. J. *Rapid Commun. Mass Spectrom.* **1993**, *7*, 614−9.
(5) Stahl, B.; Steup, M.; Karas, M.; Hillenkamp, F. *Anal. Chem.* **1991**, *63*, 1463−6.
(6) Cancilla, M. T.; Penn, S. G.; Carroll, J. A.; Lebrilla, C. B. *J. Am. Chem. Soc.* **1996**, *118*, 6736−45.
(7) Tseng, K.; Lindsay, L. L.; Penn, S. G.; Hedrick, J. L.; Lebrilla, C. B. *Anal. Biochem.* **1997**, *250*, 18−28.
(8) Harvey, D. J.; Bateman, R. H.; Green, M. R. *J. Mass Spectrom.* **1997**, *32*, 167−87.
(9) Mock, K. K.; Davey, M.; Cottrell, J. S. *Biochem. Biophys. Res. Commun.* **1991**, *177*, 644−51.
(10) Spengler, B.; Kirsch, D.; Kaufman, R.; Lemoine, J. *J. Mass Spectrom.* **1995**, *30*, 782−7.
(11) Juhasz, P.; Biemann, K. *Carbohydr. Res.* **1995**, *270*, 131−47.
(12) Stahl, B.; Thurl, S.; Zeng, J. R.; Karas, M.; Hillenkamp, F.; Steup, M.; Sawatzi, G. *Anal. Biochem.* **1994**, *223*, 218−26.
(13) Lemoine, J.; Chirat, F.; Domon, B. *J. Mass Spectrom.* **1996**, *31*, 908−12.
(14) Küster, B.; Naven, T. J. P.; Harvey, D. J. *J. Mass Spectrom.* **1996**, *31*, 1131−40.
(15) Orlando, R.; Bush, C. A.; Fenselau, C. *Biomed. Environ. Mass Spectrom* **1990**, *19*, 747−54.
(16) Lemoine, J.; Fournet, B.; Despeyroux, D.; Jennings, K. R.; Rosenberg, R.; Hoffmann, E. D. *J. Am. Soc. Mass Spectrom.* **1993**, *4*, 197−203.
(17) Ngoka, L. C.; Gal, J. F.; Lebrilla, C. B. *Anal. Chem.* **1994**, *66*, 692−8.
(18) Dell, A.; Oates, J. E.; Morris, H. R.; Egge, H. *Int. J. Mass Spectrom. Ion Phys.* **1983**, *46*, 415.
(19) Dell, A.; Morris, H. R.; Egge, H.; Nicolai, H. V.; Strecker, G. *Carbohydr. Res.* **1983**, *115*, 41−52.
(20) Dell, A. *Adv. Carbohydr. Chem. Biochem.* **1987**, *45*, 19−72.
(21) Zhou, Z.; Ogden, S.; Leary, J. A. *J. Org. Chem.* **1990**, *55*, 5444−6.
(22) Hofmeister, G. E.; Zhou, Z.; Leary, J. A. *J. Am. Chem. Soc.* **1991**, *113*, 5964−70.

10.1021/ac9813484 CCC: $18.00
Published on Web 05/29/1999

Scheme 1

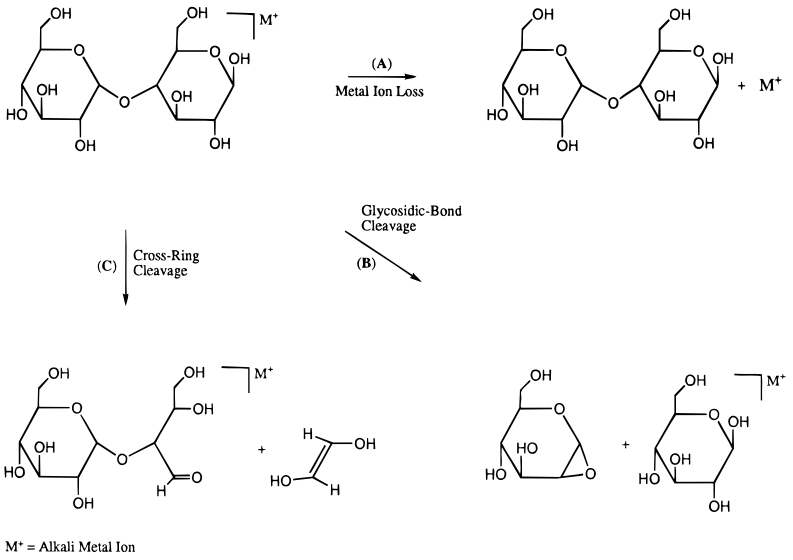

in the three reactions have been explored but not in great detail. (For clarity, "dissociation" reactions will refer to loss of the metal ion only while "fragmentation" reactions will refer to the covalent bond cleavages of the oligosaccharide.) These studies involve only ions produced primarily by fast atom bombardment (FAB) or laser desorption (LD).[21,22,25,27−29] Currently, there is a dearth of studies on the effect of alkali metal ions on MALDI-produced oligosaccharides.

The facility for loss of alkali metal ions, pathway A (Scheme 1), determines the sensitivity of the analysis. Dissociation of the cation during MALDI or CID means loss of the signal. Currently, there is very little information about the gas-phase thermodynamics of carbohydrates bound to alkali metal ions. Unlike the case of amino acids and peptides, there are no alkali metal ion affinities reported for mono- or oligosaccharides. Alkali metal ion binding to saccharides has only recently been investigated with Na^+ on a number of monosaccharides.[30] Coordination in even di- or trisaccharides is expected to differ from that in monosaccharides. Using semiempirical calculations, Leary postulates that disaccharides composed of hexoses bind Li^+ near the glycosidic linkage coordinating with as many as four oxygen atoms.[22]

Glycosidic bond cleavages (pathway B) and cross-ring cleavages (pathway C) are important for the determination of sequence and linkages, respectively. Alkali metal ion coordinated oligosaccharides produce glycosidic bond cleavages that are analogous to those observed with protonated species. Unlike protonated oligosaccharides, alkali metal ion coordinated species produce cross-ring cleavages that are highly specific to their linkages.[31−33] Cross-ring cleavages are useful for determining linkages between component monosaccharides and the branching arrangements. Cross-ring cleavages are generally not observed with protonated oligosaccharides. Mechanistic investigations involving isotopically labeled substrates by Leary and co-workers have led the authors to postulate mechanisms for glycosidic bond cleavage that involve, to some extent, the alkali metal ion.[21,22] CID studies suggest that cross-ring cleavages do not involve the charge in the cation mode and can be conceived as charge-remote fragmentation.[16,21,22]

In this paper, we propose a method for obtaining relative dissociation thresholds using multiple-collision CID. The multi-collision dissociation threshold (MCDT) values are then used to examine (1) the relative affinities of alkali metal ions for oligosaccharides and (2) the effect of alkali metal ions on oligosaccharide fragmentation, including glycosidic bond and cross-ring cleavages. The method requires obtaining threshold energies of ions whose translational energies are known. By obtaining the MCDT of various alkali metal ions, we will determine which metal is most suitable for observing quasimolecular ions by MALDI. By comparing the dissociation thresholds of cross-ring cleavages and glycosidic bond cleavages, we will determine the best alkali metal for obtaining the largest number of structurally important fragment ions. In addition, comparison of the MCDT values of different alkali metal ion complexes will provide further insight into whether fragmentation reactions are charge-site or charge-remote processes.

To obtain relative alkali metal ion binding affinities of oligosaccharides, a disaccharide (chitobiose) and a trisaccharide (chitotriose) composed of *N*-acetylglucosamines were examined. These two oligosaccharides were employed because *N*-acetyl functional groups serve as ligands that bind strongly to alkali metal ions. Di- and trisaccharides composed exclusively of hexose type sugars do not bind large alkali metal ions effectively during MALDI and subsequently do not produce abundant quasimolecular ions.[6] To investigate glycosidic bond cleavages, fucosylated oligosaccharides

(23) Hofmeister, G.; Leary, J. A. *Org. Mass Spectrom.* **1991**, *26*, 811−2.
(24) Reinhold, V. N.; Carr, S. A. *Mass Spectrom. Rev.* **1983**, *2*, 153−221.
(25) Coates, M. L.; Wilkins, C. L. *Anal. Chem.* **1987**, *59*, 197−200.
(26) Martin, W. B.; Silly, L.; Murphy, C. M.; Raley, T. J. J.; Cotter, R. J.; Bean, M. F. *Int. J. Mass Spectrom. Ion Processes* **1989**, *92*, 243−65.
(27) Spengler, B.; Dolce, J. W.; Cotter, R. J. *Anal. Chem.* **1990**, *62*, 1731−7.
(28) Teesch, L. M.; Adams, J. In *Experimental Mass Spectrometry*; Russell, D. H., Ed.; Plenum Press: New York, 1994.
(29) Coates, M. L.; Wilkins, C. L. *Biomed. Mass Spectrom.* **1985**, *12*, 424−8.
(30) Chiarelli, M. P.; Gross, M. L. *Int. J. Mass Spectrom. Ion Processes* **1987**, *1987*, 37−52.
(31) Garozzo, D.; Giuffrida, M.; Impallomeni, G.; Ballistreri, A.; Montaudo, G. *Anal. Chem.* **1990**, *62*, 279−86.
(32) Carroll, J. A.; Lebrilla, C. B. *Org. Mass Spectrom.* **1992**, *27*, 639−43.
(33) Carroll, J. A.; Willard, D.; Lebrilla, C. B. *Anal. Chim. Acta* **1995**, *307*, 431−47.

were examined because fucose glycosidic bonds readily dissociate in the cation mode. Cross-ring cleavages were examined with tetrasaccharides composed of variably linked glucoses.

EXPERIMENTAL SECTION

Materials. *N*,*N*′-diacetylchitobiose (chitobiose), *N*,*N*′,*N*″-triacetylchitotriose (chitotriose), maltotetraose, isomaltotetraose, and cellobiose were obtained from Sigma Chemical Co. (St. Louis, MO). 18-Crown-6 (18-C-6) and 2,5-Dihydroxybenzoic acid (DHB) were purchased from Aldrich Chemical Co. (Milwaukee, WI). Lacto-*N*-difucohexaose I and II (LNDFH-I and -II) and 2- and 3-fucosyllactose (2- and 3-FL) were provided by Oxford Glycosystems (Rosedale, NY). All materials were obtained in the highest purity and used without further purification.

Matrix-Assisted Laser Desorption/Ionization (MALDI). All the experiments were performed on a HiResMALDI external-source FTMS instrument (IonSpec Corp., Irvine, CA) equipped with a 4.7 T magnet in the positive-ion mode.[7] The conditions and procedures used for MALDI-FTMS are provided in several earlier publications.[6,34−37] MALDI was performed using an LSI 337 nm nitrogen laser. For the crown ethers, solutions were prepared composed of 1 mM 18-C-6 and 1 mM alkali metal chloride in water. For MALDI, 1 μL of the 18-C-6/alkali metal chloride solution was applied to a stainless steel MALDI probe tip, followed by 1 μL of DHB matrix solution (50 mg/mL in ethanol). All oligosaccharides were dissolved in water or ethanol at concentrations of approximately 1 mg/mL. For MALDI, a 1 μL aliquot of the oligosaccharide solution was applied to the probe tip, followed by 1 μL of 0.01 M alkali metal chloride in methanol and 1 μL of DHB matrix solution. All samples were allowed to crystallize rapidly on the probe tip with forced warm air.

Collision-Induced Dissociation (CID). The externally produced ions were transported through the inhomogeneous region of the magnetic field using a single-stage quadrupole rod assembly. The ions were trapped and then translationally cooled to the center of the cell by a 2 ms argon pulse. The molecular ion was isolated by ejecting all other ions from the cell with a series of on-resonance radio frequency (rf) bursts. Sustained off-resonance collision-induced dissociation (SORI CID) experiments were executed by translationally exciting the molecular ion with a 1 s rf burst at a frequency that was 1000−2000 Hz above the cyclotron frequency of the ion. During the SORI excitation event, four argon pulses (2 ms each) were applied in 250 ms intervals to maintain a constant pressure of 5×10^{-5} Torr (corrected ionization gauge pressure) followed by a 4 s delay to allow pump-down before detection.

Molecular Dynamics Calculations. Molecular modeling dynamics calculations were performed on a Silicon Graphics workstation employing the Insight II/Discover molecular modeling program package (Biosym Technologies, San Diego, CA). The AMBER force field was used for all the molecular dynamics calculations. Each alkali metal ion−oligosaccharide complex was dynamically heated at 800 K for 10 ps and then gradually cooled in 100 K increments with each lasting 5 ps to 200 K. The resulting structure was minimized to produce a 0 K structure. The complex was then reheated to 800 K, and the process was repeated to produce a second 0 K structure. The entire procedure was repeated to obtain a total of 90 structures for each oligosaccharide−alkali ion metal complex. Typically, the lowest five structures had very similar features, and the lowest of these was used as the representative structure.

To calculate the internal vibrational energy of the complexes, vibrational frequencies (in cm^{-1}) of the systems were obtained from semiemperical calculations using MNDO contained in the molecular modeling program SPARTAN (Wavefunction, Inc., Irvine, CA).

RESULTS

Determination of Multicollision Dissociation Threshold Values. Multicollision dissociation threshold (MCDT) values were determined from the kinetic energy dependence of the CID products. After the ions of interest were isolated, the ions' kinetic energy was controlled using off-resonance excitation. The translational energy of an ion during the application of a sustained off-resonance electric field is given by

$$E_{tr} = \frac{q^2E^2}{2m(\omega_1 - \omega_c)^2} \sin^2\{{}^1/_2[(\omega_1 - \omega_c)t]\} \qquad (1)$$

where E_{tr} is the translational energy of the ion, E is the amplitude of the electric field, m is the mass of the ion, q is the ion's charge, t is the time of the applied electric field, ω_1 is the frequency of the electric field, and ω_c is the ion's cyclotron frequency. Equation 1 applies to an analyzer cell with infinite length. The elongated cell used in this instrument is more akin to an infinite plate capacitor,[38] so that the equation applies without a correction factor. For a cubic cell, a correction factor must be applied to eq 1 to provide kinetic energies.[39] Since the translational energy of an ion undergoing off-resonance excitation is time dependent, the average translational energy, $\langle E_{tr}\rangle$, was used:

$$\langle E_{tr}\rangle = \frac{q^2E^2}{4m(\omega_1 - \omega_c)^2} \qquad (2)$$

The amplitude of the electric field is given by

$$E = \frac{\beta V_{pp}}{d} \qquad (3)$$

where β is a geometry factor (0.831 for a 2 in. × 2 in. × 4 in. elongated ICR cell),[40] V_{pp} is the amplitude of the applied electric field, and d is the distance between the plates (0.0508 m).

Collisional activation with off-resonance excitation increases an ion's internal vibrational energy sequentially with low-energy

(34) Cancilla, M. T.; Penn, S. G.; Lebrilla, C. B. *Anal. Chem.* **1998**, *70*, 663−72.
(35) Penn, S. G.; Cancilla, M. T.; Green, M. K.; Lebrilla, C. B. *Eur. Mass Spectrom.* **1997**, *3*, 67−79.
(36) Penn, S. G.; Cancilla, M. T.; Lebrilla, C. B. *Anal. Chem.* **1996**, *68*, 2331−9.
(37) Carroll, J. A.; Penn, S. G.; Fannin, S. T.; Wu, J.; Cancilla, M. T.; Green, M. K.; Lebrilla, C. B. *Anal. Chem.* **1996**, *68*, 1798−804.
(38) Hunter, R. L.; Sherman, M. G.; McIver, R. T., Jr. *Int. J. Mass Spectrom. Ion Processes* **1983**, *50*, 259−74.
(39) Katritzky, A. R.; Watson, C. H.; Dega-Szafran, Z.; Eyler, J. R. *J. Am. Chem. Soc.* **1990**, *112*, 2471−8.
(40) Grosshans, P. B.; Marshall, A. G. *Anal. Chem.* **1991**, *63*, 2057−61.

collisions. This occurs with multiple collisions, making it necessary to calculate the average amount of internal energy the ions obtained during the excitation period. The average translational energy converted to internal energy in the limit of infinite collisions[41] during *on-resonance* excitation is given by

$$\langle E_{cm\infty}\rangle = \frac{m_t + m_p}{m_t + 2m_p}\langle E_{tr}\rangle \quad (4)$$

where m_t is the mass of the target gas and m_p is the mass of the ion. Although the experiments performed in this work involve *off-resonance* excitation, this relationship provides a useful starting point at least for comparison. Rather than $E_{cm\infty}$, E_{com} or the center of mass energy for the first collision could have been used and would have produced the same trends. The selection of $E_{cm\infty}$ was felt to be more appropriate.

Because of limitations in the dynamic range of the instrument, it is difficult to accurately obtain threshold values. We found that an empirical equation developed by Armentrout can be used to fit the data and extrapolate the threshold.[42,43] For FTMS, the fitting function has been modified by Eyler to provide a rate constant, k_{CID}[44]

$$k_{CID} = \frac{\ln(I/I_0)}{nt} \quad (5)$$

where n is the number density of the target gas and I/I_0 is the percent fragmentation. A plot of k_{CID} vs $\langle E_{cm\infty}\rangle$ is constructed, and the data are fitted with a modified fitting function

$$k_{CID} = \frac{k_0(\langle E_{cm\infty}\rangle - E_0)^v}{\langle E_{cm\infty}\rangle^m} \quad (6)$$

where m is held constant and equal to 1 and the variables k_0, E_0 (the dissociation threshold), and v are optimized with a nonlinear least-squares analysis. Katritzky et al. used the modified form of the method (excluding $E_{cm\infty}$) to determine threshold energies of substituted phenylpyridines.[44]

It should be noted that Armentrout's method allows the determination of bond dissociation energies at 0 K and can be converted to bond enthalpies at 298 K. Originally, this method was developed for an octupole ion guide, but its successful application in quadrupole ion guides is well-known.[45] It is also commonly used with much simpler systems involving typically monodentate ligands. It has only recently been used to study alkali metal binding to amino acids and peptides using electrospray ionization (ESI).[46] The method is primarily applied in single-collision conditions and has not been applied to the multiple-collision conditions used in this study.

Extraction of MCDT values must take into account the kinetic energy spread of the ion and neutral collision gas.[39] After the ion excitation event, the kinetic energy distribution becomes broader:

$$\Delta T = (E_{ion})^{1/2}\epsilon^{1/2} + \epsilon \quad (7)$$

where E_{ion} is the kinetic energy of the ion (E_{ion} is equal to $\langle E_{tr}\rangle$ for these experiments) and $\epsilon = {}^1/_2 kT$. This correlates to a spread in the center of mass energy for a given translational energy corresponding to

$$W_{1/2,b} = \frac{m_t}{m_p + m_t}\Delta T \quad (8)$$

The effective temperature of the neutral target gas, T_b, which also takes into account the spread of the ion kinetic energies, is given by

$$kT_b = kT + \frac{(W_{1/2,b})^2}{11.1\gamma E_T} \quad (9)$$

where $\gamma = m_p/(m_p + m_t)$. The amended energy, E_T, is obtained from

$$E_T = E_0 + 0.6W_{1/2}(E_T) \quad (10)$$

where

$$W_{1/2}(E_T) = (11.1\gamma kT_b E_T)^{1/2} \quad (11)$$

After E_0 is determined from eqs 5 and 6, an initial guess of E_T is substituted into eq 10, and eqs 7−11 are iterated until duplicate values are determined for E_T. E_T is equal to the MCDT of ions with internal energies corresponding to 300 K, the formal temperature of the target gas in the ICR cell. A corrected MCDT ($MCDT_{cor}$) is provided which corresponds to the 0 K value and is obtained by accounting for the rotational and vibrational energies of the ion at 300 K. To convert MCDT to $MCDT_{cor}$, ${}^3/_2 kT$ is added to MCDT for the rotational energy of the ion. The vibrational energy for each normal mode is also added to MCDT using the equation

$$E_{vib} = \left[\frac{h\nu}{kT}\left(\frac{1}{\exp(h\nu/kT) - 1}\right)\right]RT \quad (12)$$

where h is the Plank constant, ν is the frequency of the oscillator, T is the temperature, and R is the universal gas constant. For frequencies in wavenumbers ($\nu = cm^{-1}$)

(41) Burnier, R. C.; Cody, R. B.; Freiser, B. S. *J. Am. Chem. Soc.* **1982**, *104*, 7436−41.
(42) Armentrout, P. B. In *Advances in Gas-Phase Ion Chemistry*; Adams, N., Babcock, L. M., Eds.; JAI Press Inc: Greenwich, CT, 1992; Vol. 1, p 83.
(43) Dalleska, N. F.; Honma, K.; Armentrout, P. B. *J. Am. Chem. Soc.* **1993**, *115*, 12125−31.
(44) Katritzky, A. R.; Shipkova, P. A.; Qi, M.; Nichols, D. A.; Burton, R. D.; Watson, C. H.; Eyler, J. R.; Tamm, T.; Karelson, M.; Zerner, M. C. *J. Am. Chem. Soc.* **1996**, *118*, 11905−11.
(45) Wenthold, P. G.; Squires, R. R. *J. Am. Chem. Soc.* **1994**, *116*, 6401.
(46) Klassen, J. S.; Anderson, S. G.; Blades, A. T.; Kebarle, P. *J. Phys. Chem.* **1996**, *100*, 14218−27.

$$E_{vib} = \left[\frac{1.4388\nu}{T}\left(\frac{1}{\exp(1.4388\nu/T) - 1}\right)\right]RT \qquad (13)$$

Dissociation thresholds, whether relative or absolute, are typically not obtained for ionic species as large those presented. They have also not been used for MALDI-produced ions. Similar studies by Eyler and co-workers on crown ethers used laser desorption/ionization.[47] Although the absolute thermodynamic quantities are desirable, the relative values are sufficient from the perspective of analytical mass spectrometry. For reasons that have already been mentioned, we emphasize that MCDT values are not absolute and should not be equated with appearance energies or absolute dissociation energies. In addition, oligosaccharides are multidentate ligands and the precise nature of their binding with alkali metal ions remains unknown. The ionic complexes are likely to be composed of several isostructures (metals coordinated to different binding sites), which means that any absolute value for alkali metal binding is in reality derived from an average for several possible binding arrangements.

The determination of absolute threshold values is further complicated by several factors including kinetic shift[48,49] and radiative cooling.[50,51] The values obtained in this study provide relative energies of alkali metal ion binding, as shown below. The similarities in binding of the different alkali metal ions to oligosaccharides are sufficient to minimize effects due to differences in binding. Because the detection time involves seconds after the CID event, the problems of kinetic shifts should also be minimized.[39] Instead, radiative cooling of the ion between collisions may pose a greater problem in determining the relative MCDT values. Radiative rates increase with tighter metal−ligand binding.[50,52,53] Therefore, alkali metal ions that are more strongly bound have higher radiative rates, producing more efficient cooling and in turn increasing the measured MCDT value further. This behavior could overestimate the relative dissociation thresholds for the more strongly coordinated complexes.

For the fragmentation reactions, pathways B and C (Scheme 1), the MCDT values provide relative activation barriers for the reactions. For comparison, we must assume that the reactions for all alkali metals proceed through the same mechanism during glycosidic bond and cross-ring cleavages. To ensure the same fragmentation reaction, oligosaccharide systems were selected that provided the least number of products during CID.

EVALUATION OF THE METHOD

To assess the value of the method that employs off-resonance excitation to obtain relative dissociation thresholds, experiments were performed with systems of similar complexity. Crown ethers were chosen to evaluate the method because gas-phase thermodynamic information is available from both experiment and theoretical calculations. Using the procedure described above, the MCDT values of alkali metal ions dissociating from the macrocyclic polyether 18-crown-6 (18-C-6) were determined. Previous FTMS CID results of Eyler et al.[47] and ab initio calculations by Glendening and co-workers[54] are used for comparison.

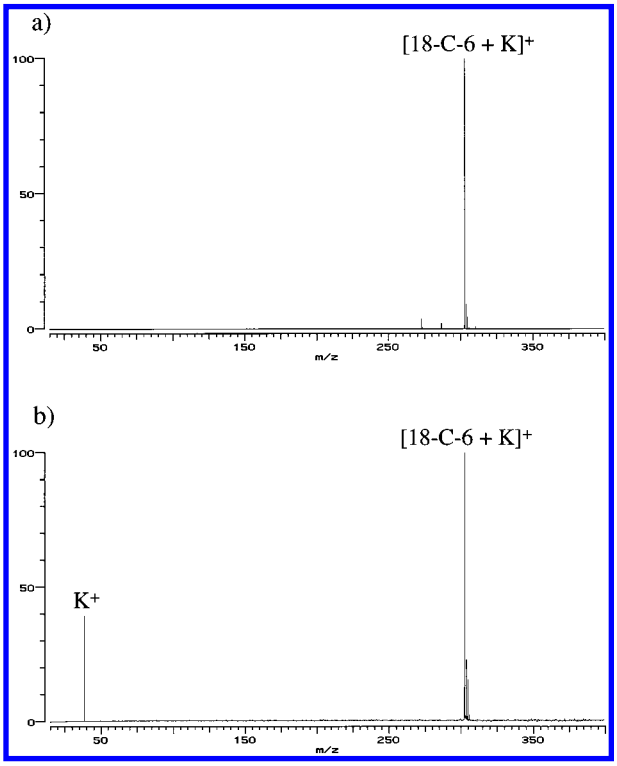

Figure 1. (a) MALDI-FTMS spectrum of [18-C-6 + K]$^+$. (b) An example spectrum of the SORI CID experiment for the determination of the MCDT of K$^+$ from the isolated quasimolecular ion in (a). The only fragmentation process observed was dissociation of the alkali metal ion.

Figure 1 shows the typical spectra obtained with 18-C-6 systems. Figure 1a is the MALDI-FTMS spectrum of 18-C-6 doped with potassium chloride. Note the lack of matrix ions or other signals that are normally observed with MALDI time-of-flight mass spectrometers at low masses. The lack of matrix ions is an important feature of the MALDI-FTMS spectrum and allows the analysis of relatively small compounds. Figure 1b is the CID of the molecular ion isolated from Figure 1a. The only CID product is the dissociation of the metal ion from the complex. This is a general behavior of all crown ethers we have examined. Covalent bond cleavages of the complexes are not observed.

The plots of CID rate constant (k_{CID}) vs $\langle E_{cm\infty} \rangle$ for 18-C-6 with various alkali metal ions are shown in Figure 2. The data from the energy-resolved CID experiments were fitted, and E_0 values were extrapolated using eqs 5 and 6. Due to limitations in the dynamic range, the lowest points on each curve correspond to only 2−4% fragmentation. The data and curve fitting functions in Figure 2 (and also Figures 6 and 7) possess the same shape as those observed in previous dissociation threshold determinations using FTMS.[44] Experimental errors were calculated from a propagation of indeterminate errors inherent in the CID experiments. The major component is due to the reproducibility of the fragmentation intensities at constant ion kinetic energies. A

(47) Katritzky, A. R.; Malhotra, N.; Ramanathan, R.; Kemerait, R. C., Jr; Zimmerman, J. A.; Eyler, J. R. *Rapid Commun. Mass Spectrom.* **1992**, *6*, 25−7.
(48) Chupka, W. A. *J. Chem. Phys.* **1959**, *30*, 191.
(49) Lifshitz, C. *Mass Spectrom. Rev.* **1982**, *1*, 309.
(50) Dunbar, R. C. *Int. J. Mass Spectrom. Ion Processes* **1983**, *54*, 109−18.
(51) Woodin, R. L.; Beauchamp, J. L. *Chem. Phys.* **1979**, *41*, 1−9.
(52) Thölmann, D.; Tonner, D. S.; McMahon, T. B. *J. Phys. Chem.* **1994**, *98*, 2002−4.
(53) Kofel, P.; McMahon, T. B. *J. Phys. Chem.* **1988**, *92*, 6174−6.
(54) Glendening, E. D.; Feller, D.; Thompson, M. A. *J. Am. Chem. Soc.* **1994**, *116*, 10657−69.

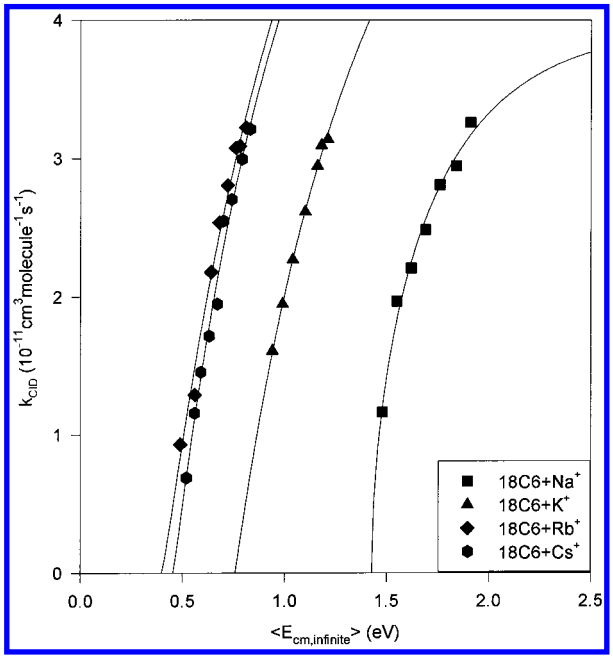

Figure 2. Plots of CID rate constants (K_{CID}) vs average ion center-of-mass kinetic energies in the limit of an infinite number of collisions ($\langle E_{cm\infty} \rangle$) for the dissociation of alkali metal ions from 18-C-6. The multicollision dissociation threshold (MCDT) values of alkali metal ions complexed to 18-C-6 were determined from the optimized fit of eqs 5 and 6.

Table 1. Multicollision Dissociation Threshold (MCDT) Values for the Dissociation of Alkali Metal Ions Bound to the Crown Ether 18-C-6[a]

guest ion	MCDT	$MCDT_{cor}$ (300 K)[b]	exptl lit. values[c,d]	theoret lit. values[e]
Na^+	1.8	2.3		3.4
K^+	1.1	1.6	1.7	3.1
Rb^+	0.8	1.3		2.5
Cs^+	0.7	1.2	1.4	2.1

[a] All values in eV. Internal energy = 0.5 eV (300 K). [b] Estimated error is ±0.2 eV. [c] Reference 43. [d] Estimated error is ±0.3 eV. [e] Reference 50.

conservative value of ±0.2 eV was obtained on the basis of multiple determinations and is consistent with earlier results obtained by FTMS.[55]

To obtain the corrected MCDT values (300 K, $MCDT_{cor}$), the internal energy is determined using a vibrational frequency analysis of the oligosaccharide. We are not aware of published vibrational frequencies for large oligosaccharides complexed to metal ions. Vibrational frequencies (cm^{-1}) were obtained from semiempirical calculations (MNDO). Internal energies were obtained from rotational and vibrational energies (eq 13) at 300 K. For 18-C-6, a value of 15 kcal mol^{-1} was obtained with MNDO. This compares well to the value of 16 kcal mol^{-1} obtained by Eyler and co-workers.[47] Both values are estimated internal energies at 350 K. The results are summarized in Table 1 along with experimental results obtained by Eyler and the theoretical results by Glendening and co-workers. There remains a large discrepancy between previous experimental results and theoretical calculations. So far, no explanation for the discrepancy has been provided. The MCDTs follow a trend consistent with the previous experimental and ab initio calculations, i.e. $Na^+ > K^+ > Rb^+ > Cs^+$. The MCDT with Li^+ could not be properly determined because of low mass limitations. Coincidentally, the MCDT values for the dissociation of K^+ and Cs^+ with 18-C-6 match those of Eyler. There is no compelling reason for the two sets of values to be identical. The previous CID studies were performed under single-collision conditions, while our method employs multiple-collision conditions. Furthermore, eq 4 has not been rigorously proven for this method or ions of this size. The purpose of this study is to obtain relative values, and in this regard the method performs satisfactorily.

Radiative cooling is a concern if various alkali metal complexes have severely different rates of radiative decay. The rates of radiative relaxation are proportional to the vibrational frequencies of the ion and decrease with the strength of the interaction. For example, the rates of radiative decay in proton-bound alcohol dimers are on the order of seconds.[56] If large variations in radiative decay exist, then even relative rates will be affected. However, on the basis of the results, we conclude that radiative decay does not significantly affect the relative rates.

Collision-Induced Dissociation of Alkali Metal Ion Coordinated Chitobiose and Chitotriose Complexes. Chitobiose (β-D-GlcNAc(1→4)D-GlcNAc) forms gas-phase complexes with all the alkali metal ions when MALDI samples are prepared with the respective alkali metal chloride. The behavior of this disaccharide composed of *N*-acetylglucosamines contrasts with that of cellobiose (β-D-Glc(1→4)D-Glc), a disaccharide composed of only glucose residues where complexes of the alkali metal ions Rb^+ and Cs^+ are not observed.

Figure 3 shows the MALDI spectra of chitobiose doped with 0.01 M CsCl. The MALDI-FTMS spectrum (Figure 3a) shows primarily the quasimolecular ion $[M + Cs]^+$ (m/z 557.079) and Cs^+ (m/z 132.907). Figure 3b shows the result of a typical CID experiment, obtained by isolation of the quasimolecular ion $[M + Cs]^+$. The only product observed corresponds to the alkali metal ion. Both the K^+ and Rb^+ quasimolecular ions behave like the Cs^+ quasimolecular ions under CID conditions.

CID of $[chitobiose + Li]^+$ exhibits a considerably more complicated spectrum (Figure 4). Glycosidic bond cleavages B_1 (or Z_1) and C_1 (or Y_1)[57] and cross-ring cleavages ($^{0,2}A_2$) are both observed (fragmentation scheme in Figure 4). Figure 4 demonstrates the detailed information that is obtained from CID of lithium-coordinated oligosaccharides.

The CID spectrum of $[chitobiose + Na]^+$ displays features that are similar to those for the Li^+-coordinated species. Figure 5 shows a plot of the relative abundance versus $\langle E_{cm\infty} \rangle$ for $[chitobiose + Na]^+$. The most facile fragmentation pathway is loss of H_2O, followed by a glycosidic bond cleavage that yields a complex with the metal ion remaining on the monosaccharide with the greater number of oxygens (C_1 or Y_1). There were two higher energy processes corresponding to another glycosidic bond cleavage (B_1 or Z_1) and cross-ring cleavage of the reducing end, $^{0,2}A_2$. The dissociation of Na^+ was not observed. It should be noted that the

(55) Bensimon, M.; Houriet, R. *Int. J. Mass Spectrom. Ion Processes* **1986**, *72*, 93.
(56) Dunbar, R. C.; McMahon, T. B.; Thölmann, D.; Tonner, D. S.; Salahub, D. R.; Wei, D. *J. Am. Chem. Soc.* **1995**, *117*, 12819−25.
(57) Domon, B.; Costello, C. E. *Glycoconjugate J.* **1988**, *5*, 397−409.

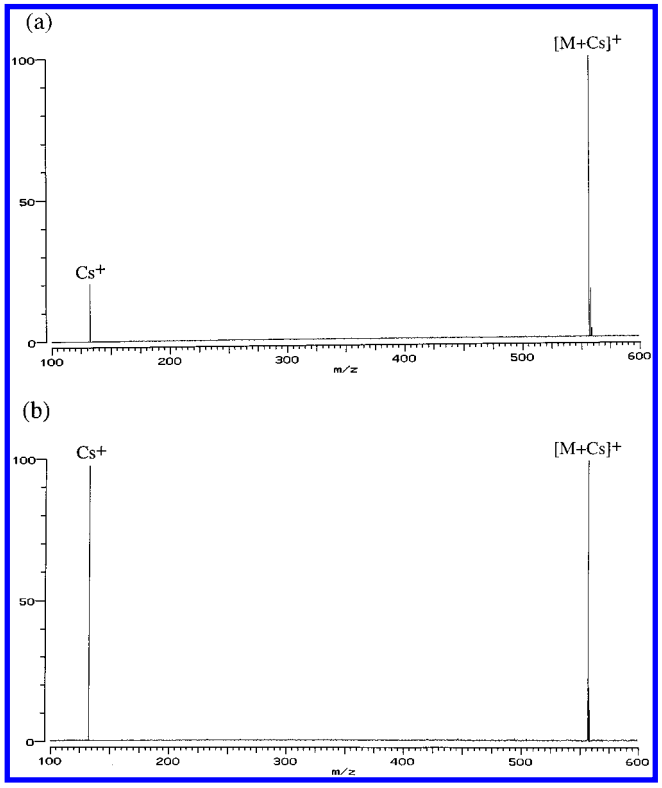

Figure 3. (a) MALDI-FTMS spectrum of [chitobiose + Cs]$^+$. (b) The MALDI-FTMS SORI CID spectrum of the isolated quasimolecular ion from (a). The only fragmentation process observed is the dissociation of the alkali metal ion.

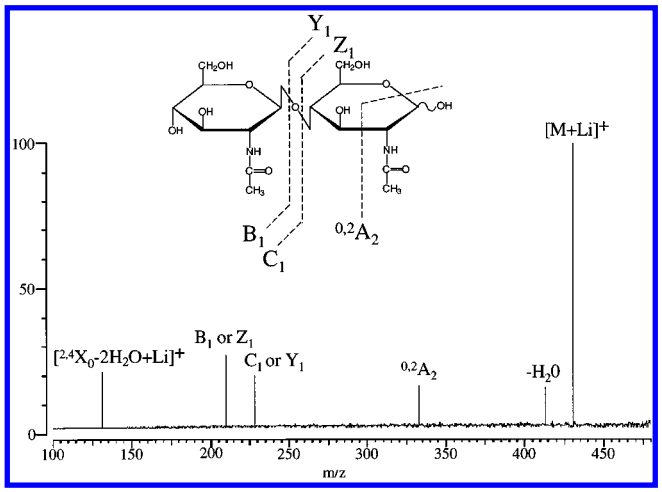

Figure 4. MALDI-FTMS SORI CID spectrum of [chitobiose + Li]$^+$. Li$^+$-coordinated chitobiose produced abundant fragmentation which yields valuable sequence information.

on-resonance CID spectrum shows primarily the loss of Na^+ as the first product (spectrum not shown). The results suggest that the dissociation of Li^+ and Na^+ from the complex proceeds through a more energetic pathway than oligosaccharide fragmentation.

The CID of the large alkali metal ions complexed to chitotriose (β-D-GlcNAc(1→4)β-D-GlcNAc(1→4)D-GlcNAc) exhibits fragmentation behavior that is similar to chitobiose, except for that of the K^+-coordinated species. The CID products correspond only to covalent bond cleavages while no bare metal ion was observed. Apparently, K^+ demonstrates a stronger coordination interaction

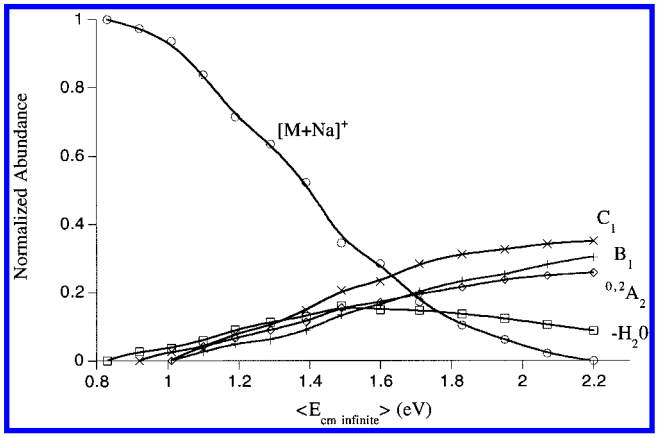

Figure 5. Reaction profile of chitobiose coordinated with Na^+. The relative abundances of the product ions are plotted as a function of $\langle E_{cm\infty} \rangle$ (eV). No appearance of the Na^+ fragment was observed.

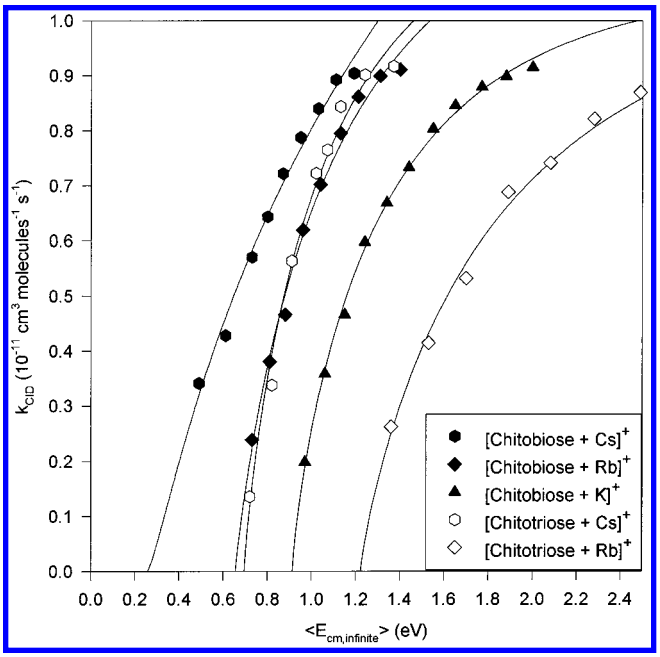

Figure 6. Plots of K_{CID} vs $\langle E_{cm\infty} \rangle$ for the dissociation of alkali metal ions from chitobiose and chitotriose.

with chitotriose than chitobiose. CID of the quasimolecular ions of [M + Li]$^+$ and [M + Na]$^+$ again produce numerous fragment ions (spectra not shown). The CID of Rb^+ and Cs^+ complexes resulted in only metal ion loss.

Dissociation Threshold Determinations of Alkali Metal Ion Complexed Chitobiose and Chitotriose. The plots of k_{CID} vs $\langle E_{cm\infty} \rangle$ for various complexes of chitobiose and chitotriose with K^+, Rb^+, or Cs^+ are shown in Figure 6. The MCDT values of alkali metal ions complexed to chitobiose and chitotriose are tabulated in Tables 2 and 3, respectively. Only MCDT values for the metal ions K^+, Rb^+, and Cs^+ could be obtained. The Na^+ complexes produced no metal loss; fragmentation of the oligosaccharide was the major process observed. The release of Na^+ was obtained only from on-resonance CID. MCDT could not be obtained using on-resonance excitation. The kinetic energies needed to produce metal ion loss under on-resonance conditions produced considerable ion loss. The MCDT values obtained for the oligosaccharides follow the same trend as those obtained for 18-C-6.

Table 2. Multicollision Dissociation Threshold (MCDT) Values of Alkali Metal Ions Bound to Chitobiose[a]

alkali metal ion	MCDT	$MCDT_{cor}$ (300 K)	alkali metal ion	MCDT	$MCDT_{cor}$ (300 K)
Cs+	0.5	1.3	Na^+	1.7−2.5[a]	2.5−3.3
Rb+	1.0	1.8	Li^+	>2.5[a]	>3.3
K+	1.3	2.1			

[a] All values in eV. Estimated error is ±0.2 eV. Internal energy = 0.8 eV (300 K). [b] Estimated; dissociation of alkali metal ion was not observed.

Table 3. Multicollision Dissociation Threshold (MCDT) Values of Alkali Metal Ions Bound to Chitotriose[a]

alkali metal ion	MCDT	$MCDT_{cor}$ (300 K)	alkali metal ion	MCDT	$MCDT_{cor}$ (300 K)
Cs+	1.0	2.1	Na^+	>1.6[b]	>2.7
Rb+	1.6	2.7	Li^+	>1.6[b]	>2.7
K+	>1.6[b]	>2.7			

[a] All values in eV. Estimated error is ±0.2 eV. Internal energy = 1.1 eV (300 K). [b] Estimated; dissociation of alkali metal ion was not observed.

Similar MCDT studies were performed using cellobiose, a disaccharide that lacks the *N*-acetyl groups of chitobiose. Rb^+ and Cs^+ complexes of cellobiose do not form in appreciable abundances with MALDI. K^+ forms abundant quasimolecular ions with cellobiose and produced the corrected MCDT (300 K) of 1.3 eV. When compared to the $MCDT_{cor}$ of K^+ from chitobiose (2.1 eV), this lower $MCDT_{cor}$ value indicates that the *N*-acetyl groups significantly increase the strength of the alkali metal−oligosaccharide interactions. It has been shown that the amide carbonyl group functions as a strong metal chelator, stronger than hydroxyls or carboxylic acids.[46] Na^+ also produced abundant quasimolecular ions with cellobiose, but again the MCDT for these complexes could not be obtained. Fragmentation of the oligosaccharide is a more energetically favorable pathway than metal ion loss. The fragmentation of Na^+-coordinated cellobiose differed slightly from that of chitobiose. Cross-ring cleavage of the reducing ring is the most favorable fragmentation pathway, followed by glycosidic bond cleavage.

There are no literature values for the strengths of interactions between alkali metal ions bound to *N*-acetylhexosamines. Using an electrospray source to produce the ions, Kebarle and coworkers obtained bond enthalpies for Na^+ and K^+ binding with simple amides, *N*-alkylamines, ketones, and carboxylic acids. Their bond enthalpies for Na^+ and K^+ binding with $MeCONMe_2$ are 1.63 and 1.26 eV, respectively.[46] The only multidentate ligand in the study, glycine, H_2NCH_2COOH, has bond enthalpies of 1.59 and 1.30 eV, respectively. In general, Na^+ bond enthalpies are found to be about 20% greater than those of the corresponding K^+. The energies of solvation of alkali metal ions by water follow a similar behavior. The dissociation energy of Na^+ coordinated to a single water molecule is almost 2 times as large as that of Cs^+. By comparison, Na^+ is only about 30% more strongly bound than K^+.[58] For 18-C-6, our relative MCDTs show that Na^+ is about 90% more strongly bound than K^+. On the basis of these results, we predict that the sodium species will have an $MCDT_{cor}$ between 2.5 and 3.3 eV for chitobiose unless there is a specific interaction related to size that favors Na^+ much more than any other alkali metal ion.

(58) Dzidic, I.; Kebarle, P. *J. Phys. Chem.* **1970**, *74*, 1466−74.

Chart 1

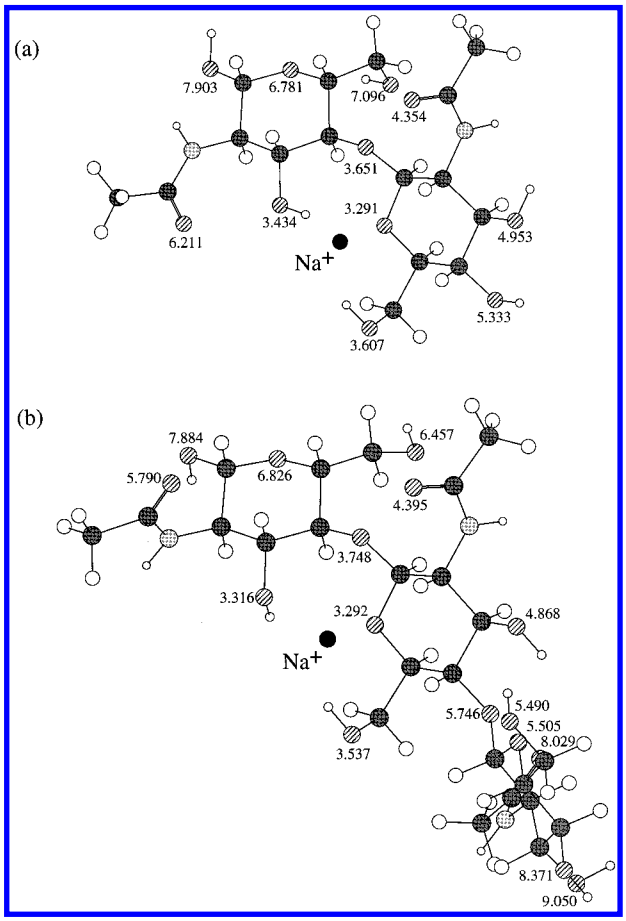

Molecular Dynamics Calculations of Alkali Metal Ion Coordinated Chitobiose and Chitotriose. To gain further insight into the possible nature of the coordination between alkali metal ions and the oligosaccharides, molecular dynamic calculations were performed on the Na^+, K^+, and Cs^+ systems. Previous molecular orbital calculations of disaccharides composed of glucoses coordinated with Li^+ predicted ligation to involve the glycosidic bond and several neighboring oxygen atoms.[22] The results of the molecular dynamics calculations are displayed in Charts 1−3. The lowest energy conformations of each system, from a total of 90 individual structures, are represented. All six structures coordinate the metal ion at or near a glycosidic oxygen. The metal is further ligated by coordination with hydroxyl, ether, and carbonyl oxygens. The distances between the oxygen atoms and the alkali metal ion are listed in each structure. An accounting of these distances in the chitobiose and chitotriose complexes provides a useful comparison of the interactions between the two oligosaccharides.

For the Na^+ species (Chart 1), the coordination sites appear similar in chitobiose and chitotriose. The binding interactions of Na^+ are maximized by the two *N*-acetylglucosamines in chitobiose. Addition of a third *N*-acetylglucosamine in chitotriose does not alter the position of the Na^+, indicating that two *N*-acetylglucosamines are sufficient to fully ligate the Na^+. The closest Na^+−O

Chart 2

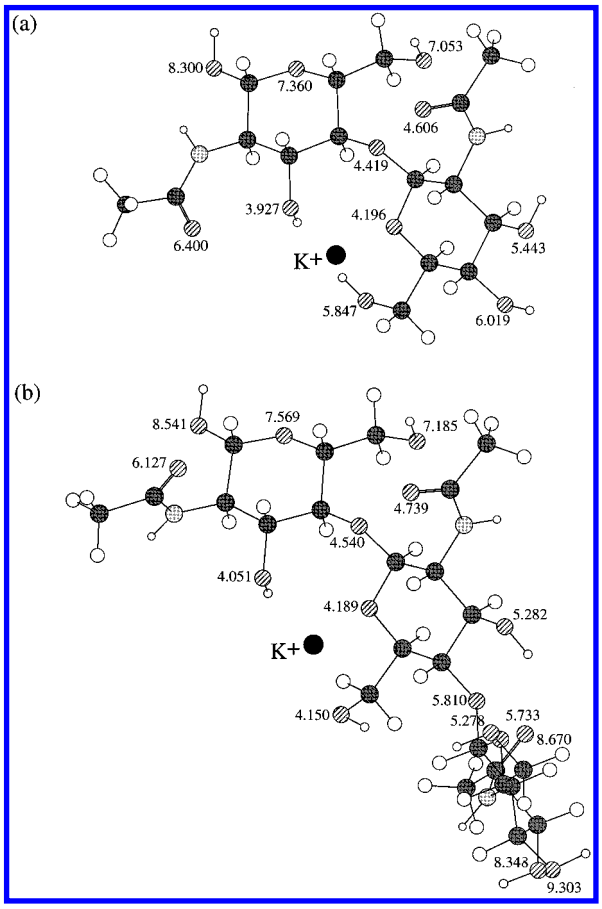

Chart 3

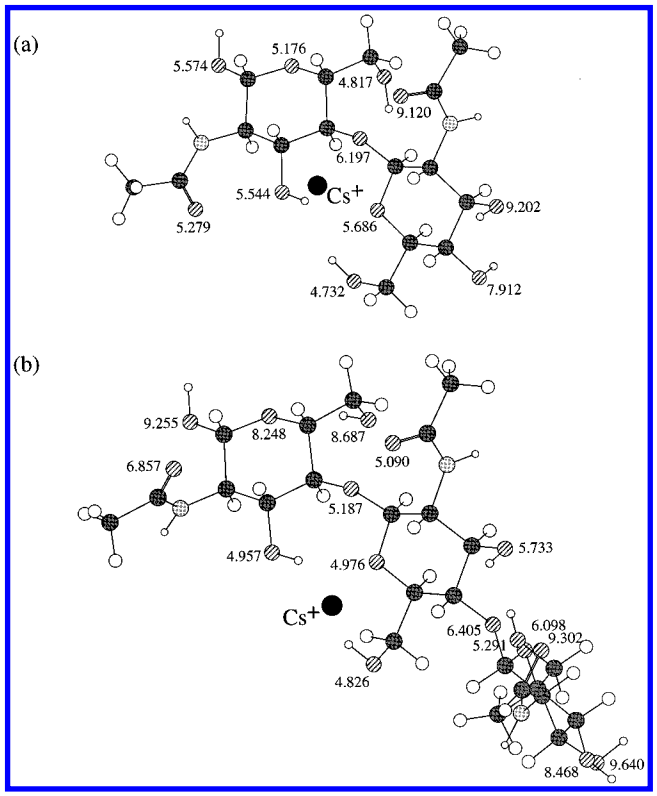

distances lie between 3.3 and 3.7 Å. For comparison, ab initio calculations predict that coordination of Na^+ to oxygens of simpler (mono- and bidentate) systems involves distances between 2 and 3 Å.[59]

When CID was performed on the quasimolecular ion $[chitotriose + K]^+$, dissociation of the metal ion was not observed, unlike the case of chitobiose. This suggests a more favorable coordination of K^+ with chitotriose than with chitobiose. The structures of the K^+-coordinated chitobiose and chitotriose are displayed in Chart 2. To assess differences in coordination between the di- and trisaccharides, the average M^+-O distances were compared. The average distances provide a measure of the extent of interaction. If the size of the molecule is increased, then the addition of more oxygen atoms will increase the average M^+-O distances. In complexes where the binding is fixed to two monosaccharide residues, the change will be greater than that in complexes where the metal attempts to also interact with the third residue. The average metal ion−oxygen distances for all six structures are tabulated in Table 4. The average K^+-O distance changes the least between chitobiose and chitotriose of the three metal ion cases studied. This suggests that the oxygens of the third *N*-acetylglucosamine of chitotriose interact better with K^+ than with Na^+ and Cs^+. This increase in the number of metal−oxygen interactions may subsequently stabilize the potassiated chitotriose quasimolecular ion compared to chitobiose.

Chart 3 illustrates the coordination of Cs^+ to chitobiose and chitotriose. The difference in average M^+-O bond distances is

Table 4. Average Alkali Metal Ion−O Distances (Å) from Charts 1−3

	av ion−O distance		
alkali metal ion	chitobiose	chitotriose	Δ (distance)
Na^+	5.147	5.769	0.622
K^+	5.779	6.220	0.441
Cs^+	6.294	6.814	0.520

0.520 Å, which lies between those for Na^+ and K^+. Cs^+ apparently interacts with the third residue more strongly than Na^+ but not as strongly as K^+. There appears to be a specific interaction between K^+ and trisaccharides. We observed similar behavior in an earlier study on the effects of alkali metal ion and the size of the oligosaccharides on the abundances of the quasimolecular ions formed by MALDI.[6]

Role of Alkali Metal Ions in Glycosidic Bond Cleavage Reactions. To determine the effect of alkali metal ions on glycosidic bond cleavages, the fragmentation of anhydrofucose was investigated. CID of fucosylated oligosaccharides produces anhydrofucose loss as the dominant fragmentation pathway. The cleavage for loss of anhydrofucose has been proposed to follow the same mechanism as hexose-type glycosidic bond cleavage.[22,60]

The experiments to investigate the loss of anhydrofucose were performed with underivatized, fucosylated oligosaccharides from two isomeric trisaccharides (2-FL and 3-FL, Chart 4) and two isomeric hexasaccharides (LNDFH-I and LNDFH-II, Chart 5). For the analysis, the product of the desired reaction channel was normalized to the sum of the total ionic species. This method is

(59) Bouchonnet, S.; Hoppilliard, Y. *Org. Mass Spectrom.* **1992**, *27*, 71−6.

(60) Fura, A.; Leary, J. A. *Anal. Chem.* **1993**, *65*, 2805−11.

Chart 4

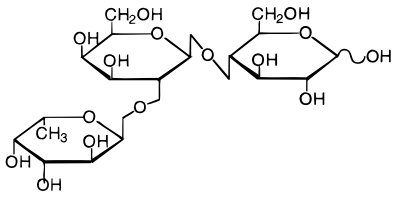

2-FL

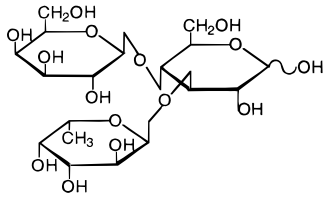

3-FL

Chart 5

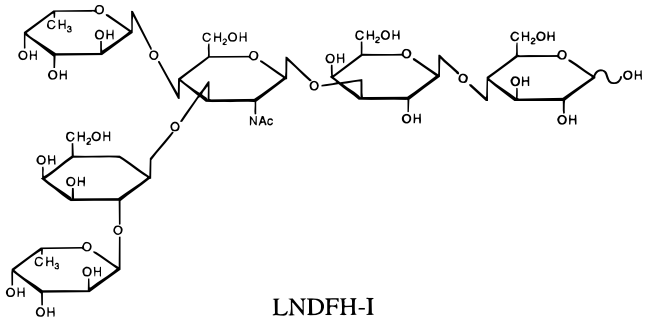

LNDFH-I

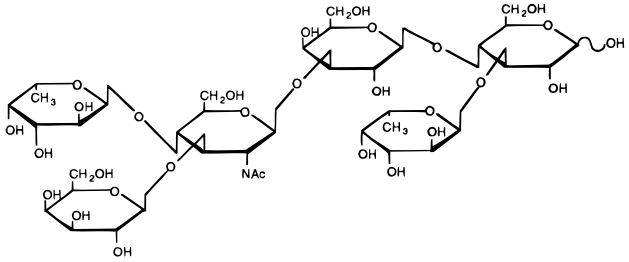

LNDFH-II

untested for multistep reaction processes, the likely mechanisms for both glycosidic bond cleavages and cross-ring cleavages. We assume that the mechanisms for these fragmentation reactions do not vary significantly between different alkali metal ions.

MALDI produced only quasimolecular ions of the FL isomers with Li^+ and Na^+. The other alkali metal ions did not form stable complexes under MALDI conditions. The corrected MCDTs for anhydrofucose loss are listed in Table 5. Due to the error range in calculating MCDTs using FTMS, we conclude no substantial energy difference between the Li^+- and Na^+-coordinated FL isomers.

Quasimolecular ions of LNDFH-I and LNDFH-II coordinated to alkali metals were all abundantly produced. When subjected to CID, even these larger difucosylated oligosaccharides lose anhydrofucose as the predominant fragmentation pathway. No other quantifiable fragments were produced until the defucosylated fragment was approximately 80% of the quasimolecular ion (spectra not shown). At larger kinetic energies, other glycosidic bond cleavages and cross-ring cleavages of the reducing end appeared. The plots of k_{CID} vs $\langle E_{cm\infty} \rangle$ for the dissociation of one anhydrofucose from the respective LNDFH-I complexes are shown in Figure 7. The resulting corrected relative MCDTs are listed in Table 5.

For the LNDFH isomers, the corrected MCDT values increase with increasing metal size. The Li^+ complexes have the lowest $MCDT_{cor}$ while the Cs^+ complexes have the highest. The variation in $MCDT_{cor}$, however, is not large. The values vary by 0.7 and 0.6 eV for LNDFH-I and LNDFH-II, respectively. These variations in dissociation thresholds should mirror similar variations in activation barriers that further translate to large differences in the rates. The variations in dissociation threshold further correspond to a 10^8-fold decrease in the rates between Li^+ and Cs^+ at 300 K.

The results suggest that glycosidic bond cleavages are facilitated by the charge carrier. Although it has been suggested that glycosidic bond cleavages are charge-remote,[61] these results are consistent with other experimental observations that suggest a charge-site process. The differences in product types between protonated and alkali metal coordinated oligosaccharides already attest to the importance of the cation in glycosidic bond cleavage.[15,28,62,63] Earlier, we have shown that Li^+-doped oligosaccharides produce greater amounts of fragments than other alkali metal ion doped oligosaccharides with both fast atom bombardment ionization and MALDI.[6,17] Metastable decay studies of various alkali metal containing oligosaccharides show that Li^+-coordinated oligosaccharides have the highest dissociation rates. Furthermore, the rates follow the order $Li^+ > Na^+ > K^+ > Rb^+ > Cs^+$.[17] In the negative-ion mode, the loss of anhydrofucose is less pronounced than that in the positive-ion mode. Papac et al. has produced MALDI-MS spectra of fucosylated, acidic oligosaccharide ions that are devoid of fucose loss.[64]

Collisional Thermalization and Radiative Decay. The sizes of the LNDFH isomers raise concerns of whether the MALDI-produced ions are vibrationally thermalized before the CID event. Ions that are not vibrationally thermalized will produce lower MCDTs. In all experiments, the MALDI-produced ions are first trapped in the analyzer cell and are then translationally and vibrationally thermalized using a 2 ms pulse of argon, which produces a maximum pressure of 5×10^{-5} Torr in the ICR cell.

To determine whether the ions are sufficiently thermalized before the CID event, the number of argon pulses was varied to increase the number of collisions prior to CID. The experiments were performed using LNDFH-I and -II coordinated with Li^+ and Na^+. The results, listed in Table 6, show no significant effect on $MCDT_{cor}$ with increasing number of pulsed gas events. The $MCDT_{cor}$ values of Li^+- and Na^+-coordinated oligosaccharides do not vary significantly. From these results, one can assume that either a single Ar pulse is sufficient to thermalize the ions or three Ar pulses are not sufficient to thermalize the ions and the ions remain in highly vibrationally excited states.

Alternatively, extending the delay time prior to the CID event may allow the ions sufficient time to thermalize. To investigate

(61) Vine, J.; Brown, L.; Boutagy, J.; Thomas, R.; Nelson, D. *Biomed. Mass Spectrom.* **1979**, *6*, 415.

(62) Cerny, R. L.; Tomer, K. B.; Gross, M. L. *Org. Mass Spectrom.* **1986**, *21*, 655−60.

(63) Teesch, L. M.; Adams, J. *Org. Mass Spectrom.* **1992**, *27*, 931−43.

(64) Papac, D. I.; Wong, A.; Jones, A. J. S. *Anal. Chem.* **1996**, *68*, 3215−23.

Table 5. Multicollision Dissociation Threshold (MCDT) Values for the Loss of Anhydrofucose from Two Isomeric Fucosylated Oligosaccharides[a]

alkali metal ion	2-FL[b] MCDT	2-FL[b] $MCDT_{cor}$ (300 K)	3-FL[b] MCDT	3-FL[b] $MCDT_{cor}$ (300 K)	LNDFH-I[c] MCDT	LNDFH-I[c] $MCDT_{cor}$ (300 K)	LNDFH-II[c] MCDT	LNDFH-II[c] $MCDT_{cor}$ (300 K)
Li^+	1.3	2.2	1.1	2.0	2.4	4.2	2.3	4.1
Na^+	1.4	2.3	1.3	2.2	2.5	4.3	2.5	4.3
K^+	NO[d]		NO		2.8	4.6	2.8	4.6
Rb^+	NO		NO		2.9	4.7	2.8	4.6
Cs^+	NO		NO		3.1	4.9	2.9	4.7

[a] All values in eV. Estimated error is ±0.2 eV. [b] Calculated internal energy = 0.9 eV (300 K). [c] Calculated internal energy = 1.8 eV (300 K). [d] NO: quasimolecular ion not observed.

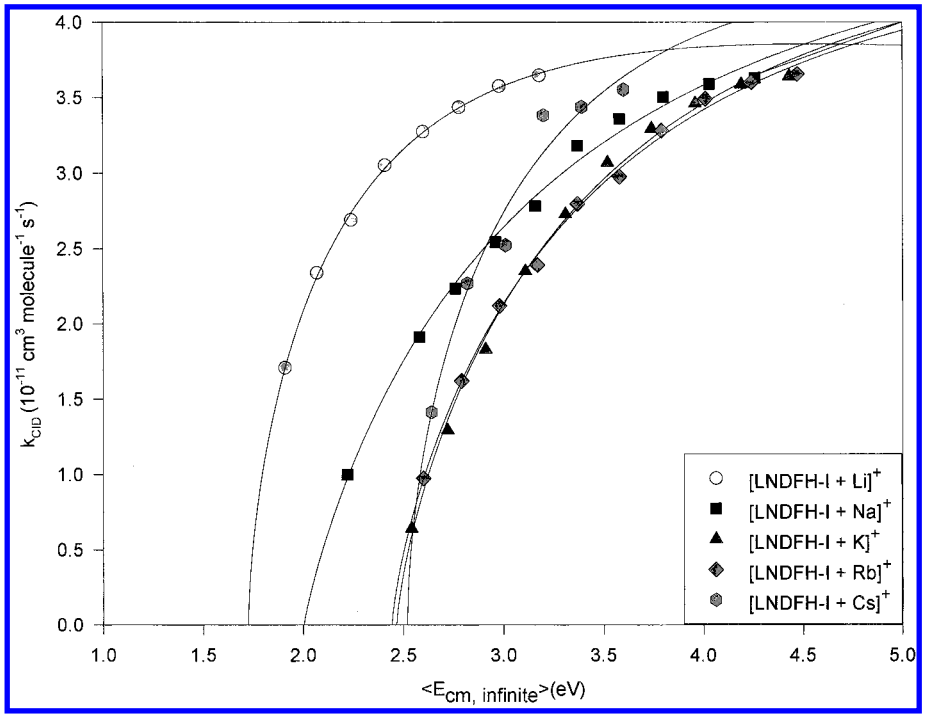

Figure 7. Plots of K_{CID} vs $\langle E_{cm\infty} \rangle$ for the loss of anhydrofucose from alkali metal ion coordinated LNDFH-I. MCDT values for the loss of anhydrofucose from the quasimolecular ion were determined from the optimized fit of eqs 5 and 6.

Table 6. Corrected Multicollision Dissociation Threshold ($MCDT_{cor}$, 300 K) Values for the Loss of Anhydrofucose as a Function of the Number of Cooling Argon Pulses before the CID Event[a]

no. of Ar pulses	LNDFH-I + Li^+	LNDFH-II + Li^+	LNDFH-I + Na^+	LNDFH-II + Na^+
1	4.1	3.9	4.4	4.3
2	4.0	3.9	4.3	4.3
3	4.3	4.1	4.4	4.2

[a] All values in eV. Estimated error is ±0.2 eV.

Table 7. Corrected Multicollision Dissociation Threshold ($MCDT_{cor}$, 300 K) Values for the Loss of Anhydrofucose from LNDFH-I Coordinated to Na^+ as a Function of Time Delay between Ion Accumulation and CID Event[a]

time (s)	$MCDT_{cor}$ (eV)	time (s)	$MCDT_{cor}$ (eV)
2.5	4.1	7	4.1
3	4.1	9	4.2
5	4.1		

[a] Estimated error is ±0.2 eV.

the possibility of long-lived vibrationally excited species, the CID event was delayed for several seconds and the $MCDT_{cor}$ was determined. The results are tabulated in Table 7, for LNDFH-I coordinated to Na^+. During a period lasting between 2 and 9 s, there was no observable change in the relative $MCDT_{cor}$ values. From these results, we conclude that the ions are vibrationally thermalized before the dissociation processes.

Energetics of Cross-Ring Cleavage Reactions. The relative MCDTs of the cross-ring cleavages were examined for two differently linked oligosaccharides, maltotetraose and isomaltotraose, with structures α-D-Glc(1→4)α-D-Glc(1→4)α-D-Glc(1→4)-D-Glc and α-D-Glc(1→6)α-D-Glc(1→6)α-D-Glc(1→6)D-Glc, respectively. A representative CID spectrum of [maltotetraose + $Na]^+$ near the dissociation threshold produces predominantly a single product at m/z 629.190 ($^{0,2}A_4$) (Figure 8a). At large translational energies, the cross-ring cleavages increase further and glycosidic bond cleavages appear (Z_3 or C_3, m/z 509.146; Y_3 or B_3, m/z 527.157) along with the loss of H_2O (m/z 671.196) (Figure 8b).

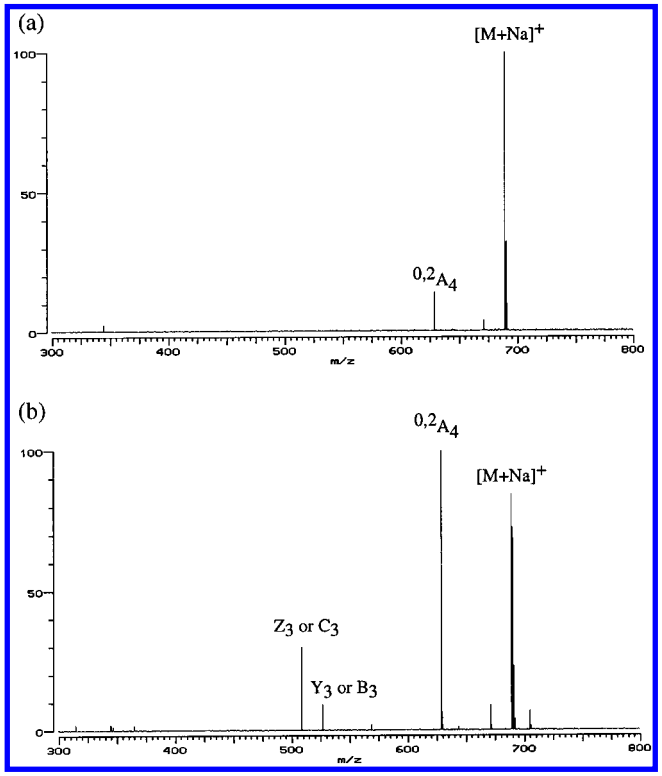

Figure 8. MALDI-FTMS CID spectra of sodiated maltotetraose (a) at just above the dissociation threshold demonstrating that the lowest energy fragment is loss of $C_2H_4O_2$ and (b) at higher translational energy.

Table 8. Multicollision Dissociation Threshold Values for the Cross-Ring Cleavage Corresponding to the Loss of $C_2H_4O_2$ (−60 u) from the Respective Quasimolecular Ion[a]

	maltotetraose[b]		isomaltotetraose[b]	
alkali metal ion	MCDT	$MCDT_{cor}$ (300 K)	MCDT	$MCDT_{cor}$ (300 K)
Li^+	1.6	2.8	1.3	2.5
Na^+	1.6	2.8	1.3	2.5
K^+	1.7	2.9	1.2	2.4
Rb^+	*c*		*c*	
Cs^+	*c*		*c*	

[a] All values in eV. Estimated error is ±0.2 eV. [b] Calculated internal energy = 1.2 eV (300 K). [c] Metal ion loss is the predominant dissociation pathway.

For a 1−6-linked oligosaccharide such as isomaltotetraose, three cross-ring cleavage products are typically observed: loss of 60, 90, and 120 u.[22,32] For a 1−4-linked oligosaccharide such as maltotetraose, two cross-ring products are observed: loss of 60 and 120 u. The different cross-ring products do not have similar MCDTs. For example, the loss of 90 and 120 u for isomaltotetraose and the loss of 120 u for maltotetraose all have greater MCDTs than loss of 60 u. The loss of $C_2H_4O_2$ is always observed as the lowest energy product for both tetrasaccharides. Therefore, to characterize the MCDTs of cross-ring cleavages, the product corresponding to the loss $C_2H_4O_2$ was selected.

The $MCDT_{cor}$ values for the loss $C_2H_4O_2$ are listed in Table 8. CID of Rb^+- and Cs^+-coordinated maltotetraose and isomaltotetraose resulted only in the loss of the metal ions. Unlike the case of glycosidic bond cleavages, there are apparently little variations in the values for cross-ring cleavages. The values range only 0.1 eV, which falls below the experimental error. The lack of correlation between the MCDTs and the size of the metal ion suggests that cross-ring cleavages are charge-remote processes. These results are consistent with the series of retro-aldol reactions, which are believed to be charge-remote processes, proposed by several researchers as mechanisms for cross-ring cleavages.[22,25,27,29] In general, we believe that all cross-ring cleavages are charge-remote and independent of the metal ion. The exceptions are cross-ring cleavages observed in the anion mode which appear to be facilitated by the negative charge.[33]

Comparison of the MCDTs between maltotetraose and isomaltotetraose produced a measurable difference for the loss of $C_2H_4O_2$. The 1−6-linked isomaltotetraose has an average $MCDT_{cor}$ that is approximately 0.4 eV lower than that of the 1−4-linked maltotetraose. The results are consistent with the notion that cross-ring cleavages are instead a function of linkage type.

CONCLUSION

For the purpose of analyzing oligosaccharides by mass spectrometry, the choice of the coordinating alkali metal ion is crucial to the overall outcome. A semiquantitative investigation of the three dissociation pathways leads to a better understanding of the role of the alkali metal ion in these processes. CID of oligosaccharides complexed to Li^+ or Na^+ minimizes metal ion dissociation (pathway A, Scheme 1) and maximizes the yields of glycosidic bond and cross-ring cleavages (pathways B and C, Scheme 1). Cs^+ and Rb^+ generate relatively weak interactions with oligosaccharides in the gas phase. When these complexes are subjected to CID, metal ion loss is the dominant fragmentation pathway and minimal sequencing information is obtained. CID of K^+ complexes produces both metal ion loss and fragmentation of the oligosaccharide. For compounds larger than trisaccharides, fragmentation is the dominant result while for smaller oligosaccharides only metal ion loss is observed.

Glycosidic bond cleavages are likely to be charge-induced processes. Li^+-coordinated oligosaccharides have the lowest activation barrier for dissociation. Li^+ may be more intimately involved in these cleavage reactions while mimicking the high charge density of a proton. However, the advantages of Li^+ in CID are counteracted by its behavior during MALDI. Samples doped with lithium salts yield a high degree of fragmentation during ionization, making the identification of the quasimolecular ion difficult. Conversely, Cs^+ is best suited for the production of quasimolecular ions. The characteristics of Cs^+ complexes have been exploited by Tseng et. al., where unknown fucosylated oligosaccharides from biological mixtures were elucidated from their fragments in the mass spectrum by forming Cs^+-coordinated ions in MALDI.[7] A compromise for obtaining strong quasimolecular ions and abundant structurally informative fragment ions is Na^+. Fortunately, this metal ion is also the most common contaminant in most biological samples.

MCDTs for cross-ring cleavages are independent of the alkali metal ion. Cross-ring cleavages are therefore charge-remote processes. However, individual cleavage products (e.g., loss of 60 u, 90, 120, etc.) have different MCDTs. Even identical products (e.g., loss of 60) may have different MCDTs if they are produced

from different linkages. Further investigations into the MCDTs of different products with different linkages are needed.

The direct comparison of activation energies between the different reactions, though desirable, is not possible with this method. Although all three reactions, metal ion loss, glycosidic bond cleavage, and cross-ring cleavage, are in direct competition during activation, they each involve fairly complex reaction mechanisms. Both fragmentation pathways involve a series of rearrangements that make the rates highly dependent on both the activation barrier and the preexponential factor. For rearrangement reactions, the preexponential factors are considerably lower than for simple bond dissociation. There have been suggestions that cross-ring cleavages require more energy than glycosidic bond cleavages because presumably more bonds are broken in the former than in the latter.[15] This notion is not always correct. In the selected example of maltotetraose and isomaltotetrase, cross-ring cleavage is clearly the more favorable fragmentation reaction.

ACKNOWLEDGMENT

Funding from the National Institutes of Health, the National Science Foundation, and the University of California, Davis, is gratefully acknowledged.

Received for review December 4, 1998. Accepted April 26, 1999.

AC9813484